










CASE REPORT

Usher syndrome and Nebulin-associated myopathy in a single patient due to variants in *MYO7A* and *NEB*

Nuno Maia^{1,2}  | Ana Rita Soares³  | Ana Maria Fortuna^{2,3}  | Isabel Marques^{1,2}  |
Ana Gonçalves^{1,2}  | Rosário Santos^{1,2}  | Manuel Melo Pires⁴  |
Arjan P. M. de Brouwer⁵  | Paula Jorge^{1,2} 

¹Unidade de Genética Molecular, Centro de Genética Médica Jacinto de Magalhães (CGM), Centro Hospitalar Universitário do Porto (CHUP), Porto, Portugal

²Unidade Multidisciplinar de Investigação Biomédica (UMIB), Instituto de Ciências Biomédicas Abel Salazar (ICBAS), Universidade do Porto, Porto, Portugal

³Unidade de Genética Médica, Centro de Genética Médica Jacinto de Magalhães (CGM), Centro Hospitalar Universitário do Porto (CHUP), Porto, Portugal

⁴Serviço de Neuropatologia, Centro Hospitalar e Universitário do Porto (CHUP), Porto, Portugal

⁵Department of Human Genetics, Donders Institute for Brain, Cognition and Behaviour, Radboud University Nijmegen, Nijmegen, The Netherlands

Correspondence

Paula Jorge, Praça Pedro Nunes, nº88, 4099-028 Porto, Portugal.
Email: paulajorge.cgm@chporto.min-saude.pt

Funding information

Centro Hospitalar Universitário do Porto, Grant/Award Number: 2017 PhD DEFI-CHUP and DEFI - 2015 (145/12) grants; Fundação para a Ciência e a Tecnologia, Grant/Award Number: UID/Multi/00215/2019

Abstract

In a patient with Usher syndrome and atypical muscle complaints, we have identified two separate variants in *MYO7A* and *NEB* genes by exome sequencing. The homozygous variants in these two recessive genes could explain the full phenotype of our patient.

KEYWORDS

homozygosity mapping, *MYO7A*, *NEB*, Nebulin-associated myopathy, Usher syndrome

1 | INTRODUCTION

Genome-wide technologies enable the identification of potentially causal variants in human disease and establish coherent genotype-phenotype associations, particularly in conditions with complex clinical presentation and genetic heterogeneity,¹⁻⁴ with a thorough interpretation of causality due to incomplete penetrance, mosaicism, or variable disease expression.^{1,4-10} Homozygosity mapping proved invaluable in identifying variants in recessive Mendelian diseases, particularly in consanguineous families.^{11,12} Although rare, phenotypic heterogeneity of typical Mendelian segregating disorders, caused by combined effects in several genes, has been previously described.^{4,10} Yet, 44 diseases caused by 213 digenic combinations, involving 136 genes and 364 pathogenic variants, are described at the digenic diseases database (DIDA, <https://omictools.com/dida-2-tool>, accessed 7 May 2020).¹³ Herein, we report a 16-year-old male patient, born to consanguineous parents, presenting with a clinical phenotype resembling Usher Syndrome.⁹ Besides ocular and hearing impairments, a history of mild skeletomuscular involvement was within his medical file. Since the latter is usually absent in Usher patients, we hypothesized that mutations in two genes could underlie the patient's phenotype. Following exome sequencing, further investigation of variants in morbid genes pinpointed to nine putatively pathogenic variants on chromosomes 2, 11, and X. Further *in silico* studies suggest that Usher disease phenotype is due to a variant in *MYO7A* modified by a Nebulin-associated myopathy, caused by a homozygous pathogenic variant in *NEB* gene.

2 | CASE REPORT

The proband is the oldest child of first-cousin healthy parents (Figure 1A). His sister is healthy, and there is no relevant family history. At 16 years of age, he was referred to the genetics clinic presenting with sensorineural hearing loss (HP:0000407) and retinitis pigmentosa (HP:0000510). He was born by eutocic delivery after full-term uncomplicated pregnancy, and showed normal somatometric parameters. He had no other symptoms except for muscular hypotonia (HP:0001252). At 4 months (mo), he was diagnosed with congenital, profound sensorineural bilateral hearing loss (HP:0008527), with the absence of auditory evoked potentials (HP:0006958). He has never accepted hearing aids. The patient's developmental milestones were smiling at 5 mo, cervical control at 8 mo, sitting at 15 mo, and independent walking at 36 mo. He was diagnosed with a global developmental delay (HP:0001263) and severe language impairment (HP:0002463) by a developmental psychologist. He always had special education support. At 2.5 years, the muscular hypotonia was still noticed by the neurologist. Brain MRI performed then revealed wide subarachnoid space (HP:0012704) and mild operculum delay. He also showed mild failure to thrive (HP:0001508), from which he had recovered by age 4. At 15 years old, he presented with decreased visual acuity (HP:0007663). Although uncooperative during the observation in the ophthalmologic clinic, he was shown to have low visual accuracy, nyctalopia (HP:0000662), bilateral retinitis pigmentosa, and cataract (HP:0000518) on the right eye. After assessment in the neuromuscular clinic, a

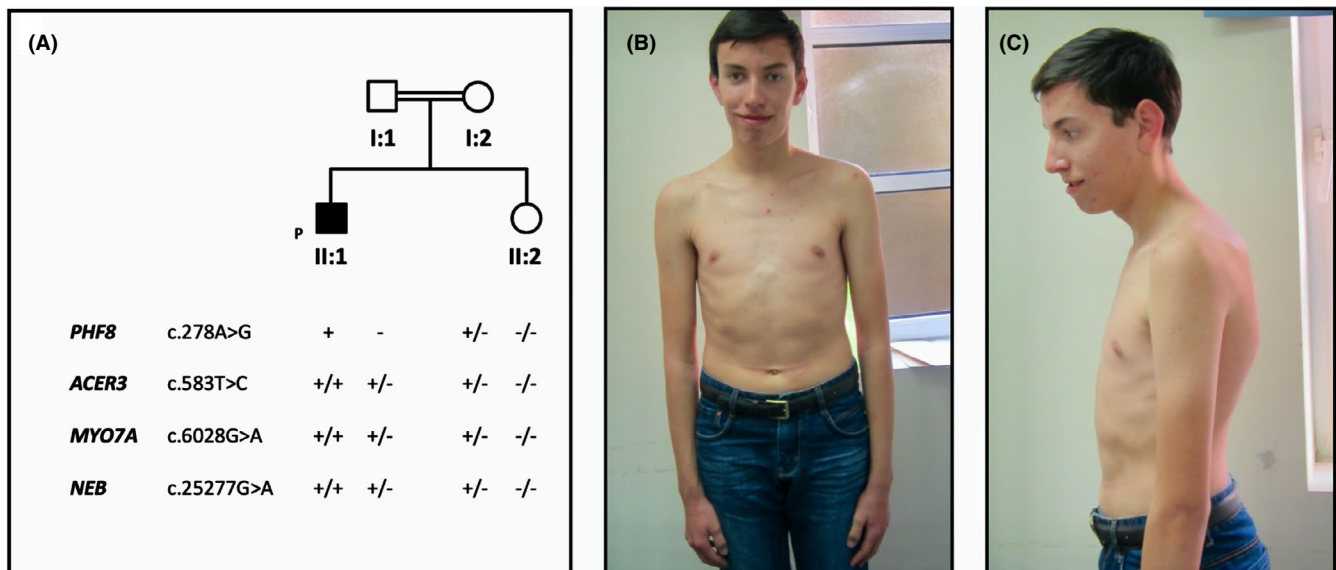


FIGURE 1 Proband's pedigree and clinical images at the age of 16 y. A, Segregation of the missense variants in *PHF8* (NM_001184896.1:c.278A>G), *ACER3* (NM_018367.6:c.583T>C), *MYO7A* (NM_000260.3:c.6028G>A), and *NEB* (NM_001271208.1:c.25277G>A) (for each gene from left to right: proband, father, mother, and sister), where “+” indicates presence and “-” absence of each variant per allele. B, Mild facial asymmetry, telecanthus, and hypertelorism. C, Ears with underfolded helix and large lobe, prognathism, and kyphosis

mild flexor weakness of the neck (HP:0003722) was identified and he is currently on a waiting list for muscle biopsy. The consequent referral to the medical genetics clinic demonstrated minor dysmorphisms with mild facial asymmetry (HP:0000324), telecanthus (HP:0000506) and hypertelorism (HP:0000316) (Figure 1B), ears with under folded helix (HP:0008577) and large earlobe (HP:0009748), high narrow palate (HP:0002705) with dental crowding (HP:0000678), mandibular prognathia (HP:0000303), and kyphosis (HP:0002808) (Figure 1C). Normal genetic investigations included conventional karyotype, *FMR1* CGG repeat number analysis, and sequencing of *GJB2* and *MED12* genes. Multiplex ligation-dependent probe amplification analysis of subtelomeric regions and microdeletion/microduplication syndromes revealed a normal copy number for all probes. No pathogenic variant was identified in a panel of 175 variants, coded by 14 genes implicated in syndromic congenital deafness. Metabolic screening of very-long-chain fatty acids, phytanic and pristanic acids, and carbohydrate-deficient transferrin was within reference values. The initial clinical diagnosis was Usher Syndrome although his full phenotypic spectrum could not be explained.

3 | METHODS

Proband's phenotypic abnormalities were described following the Human Phenotype Ontology Project (HPO; <https://hpo.jax.org/app/>) terminology.^{14,15} Exome sequencing (ES) analysis was performed on proband's blood sample genomic DNA (gDNA) obtained by salting-out.¹⁶ Exome libraries were captured using SureSelect V5-post Kit (Agilent Technologies, Santa Clara, CA, USA), and 100-bp paired-end sequencing was performed using the Illumina HiSeq 2000/2500 (Illumina, San Diego, CA, USA). Raw data of FASTQ file format were assembled into the University of California Santa Cruz (UCSC) Genome Browser using genome analysis toolkit (GATK v3.4.0) (<http://genome.ucsc.edu/>; hg19 - NCBI build GRCh37), and variants were annotated using SnpEff (SnpEff_v4.1g).¹⁷ Variants passing following filters were selected for clinical correlation: (a) frequency <1% (dbSNP, GnomAD Browser, and local databases); (b) gene component, that is, exon and canonical splice acceptor or donor sites; (c) nonsynonymous consequence; and (d) *in silico* deleteriousness and spliceogenic effect predictions, using tools: (i) combined Annotation Dependent Depletion scoring (<http://cadd.gs.washington.edu/score>; CADD threshold ≥ 15)¹⁸; (ii) SpliceSiteFinder-like (SSF, normal score threshold ≥ 70 for SDS and SAS)¹⁹; (iii) MaxEntScan (MES, normal score threshold ≥ 0 for SDS and SAS)²⁰; (iv) NNSPLICE (NNS, normal score threshold ≥ 0.4 for SDS and SAS)²¹; and (v) GeneSplicer (GS, normal score threshold ≥ 0 for SDS and SAS).²² Variant nomenclature

follows the Human Genome Variation Society (HGVS) recommendations (<http://hgvs.org/mutnomen/>).²³ The putative candidate variants were validated and assessed for familial segregation analysis by Sanger sequencing using gDNA isolated from peripheral blood samples from parents, sister and a second blood sample from the proband. Briefly, symmetric PCR products were purified using the Illustra™ ExoStar™ 1-Step (GE Healthcare Life Sciences®, Little Chalfont, UK), sequenced using the BigDye® Terminator v3.1 cycle sequencing kit (Applied Biosystems™), and further analyzed with SeqScape Software v2.5 (Applied Biosystems™). We used the human androgen receptor gene assay (HUMARA) to determine the X-chromosome inactivation (XCI) pattern in proband's mother gDNA sample.²⁴ The XCI ratio obtained after digestion with *HhaI* methylation-sensitive endonuclease is calculated dividing the percentage of methylation of allele 1 by allele 2; [80:20] random; [90:10] highly skewed; and [100:0] completely skewed.²⁵

4 | RESULTS

The initial variant filtering was restricted to the X-chromosome and large autozygous regions given the parental consanguinity, allowing the identification of nine putative pathogenic variants (Table S1). We identified only one X-linked variant, in *PHF8* gene (OMIM*300560), NM_001184896.1:c.278A>G, p.(His93Arg) (Figure 1A). This hemizygous missense variant is present in the PHF8 demethylase domain a highly conserved amino acid, juxtaposed to the plant homeodomain finger domain. Pathogenic *PHF8* variants are implicated in Siderius X-linked mental retardation syndrome (MRXSSD, OMIM#300263).²⁶⁻²⁸ Patients affected with MRXSSD show broad assiduous features like developmental delay, dysarthric speech and developmental impairment, and typical dysmorphic features, absent in our proband, such as cleft lip/palate, preaxial polydactyly, large hands and cryptorchidism. *PHF8* c.278A>G variant, with a CADD score of 24.3, is maternally inherited and is classified in ClinVar as variant of unknown significance (VOUS) (Table S1). A normal X-chromosome inactivation (XCI) pattern [85:15] was identified in our proband's mother blood sample. A complete skewing of the XCI pattern has been previously reported in the majority of *PHF8* carrier mothers.^{26,28} Using a homozygous cutoff ratio above 85%, SNP autozygosity mapping was assessed based on exome data (Figure 2). Two large autozygous regions at chromosome 2 (g.136873549 - g.213886454) and chromosome 11 (g.136873549 - g.78776192), were observed (Table S1). Within these regions, putative homozygous pathogenic variants were identified in *LRPIB* (OMIM*608766), *NMI* (OMIM* 603525) and *NEB* (OMIM*161650), *ANAPC15* (OMIM* 614717), *ACER3* (OMIM*617036) and *MYO7A* (OMIM*276903) genes (Table S1), but only those identified

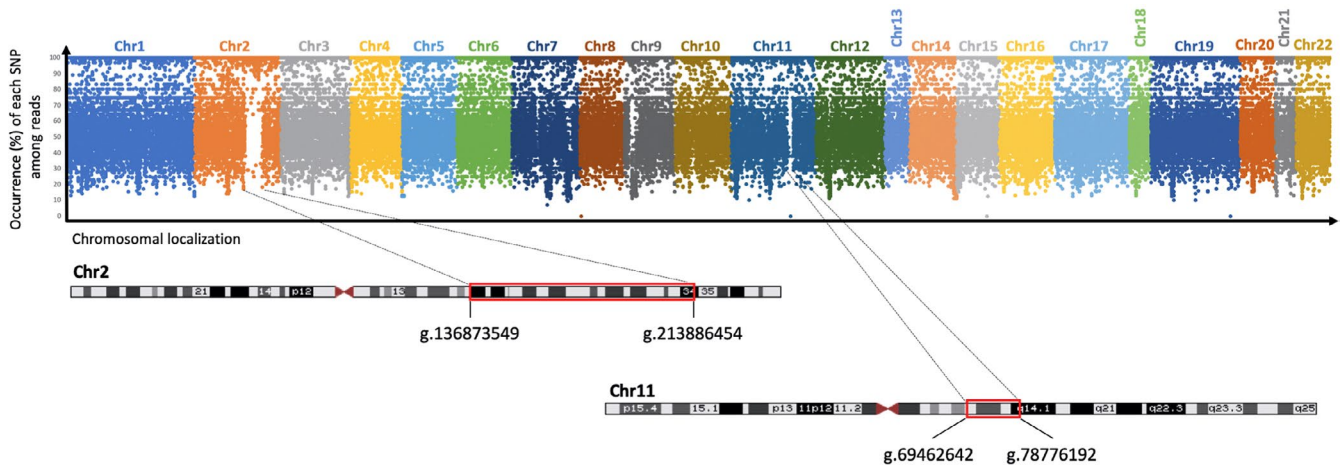


FIGURE 2 Manhattan plot of the occurrence (%) of single nucleotide polymorphisms (SNPs) among the autosomes. Each dot stands for a variant where each color represents a different autosome (indicated above of the plot). A significant number of contiguous SNPs with a percentage of occurrence >85% result in gaps. In chromosomes 2 and 11 ideograms (extracted from UCSC genome browser⁴⁰), the homozygosity regions are represented as red rectangles with the respective bordering genomic coordinates

within morbid genes, namely *ACER3*, *MYO7A*, and *NEB*, were further analyzed. The identified homozygous missense variant NM_018367.6:c.583T>C, p.(Phe195Leu) in *ACER3* gene is not described in gnomAD and affects a highly conserved amino acid residue. *ACER3* pathogenic variants are the underlying cause of Early Childhood-onset Progressive Leukodystrophy (PLDECO, OMIM#617762), a gradual condition affecting the central nervous system with leukodystrophy

and cerebral atrophy. Dysmorphic features, such as coarse facies and macrocephaly, together with developmental regression, severe intellectual disability, absence of language are described in PLDECO.²⁹ None of these severe clinical features are observed in our proband, corroborated by MRI analysis. Two homozygous missense variants were identified in *MYO7A* gene, NM_000260.3:c.1007G>A, p.(Arg336His) and NM_000260.3:c.6028G>A, p.(Asp2010Asn), despite a

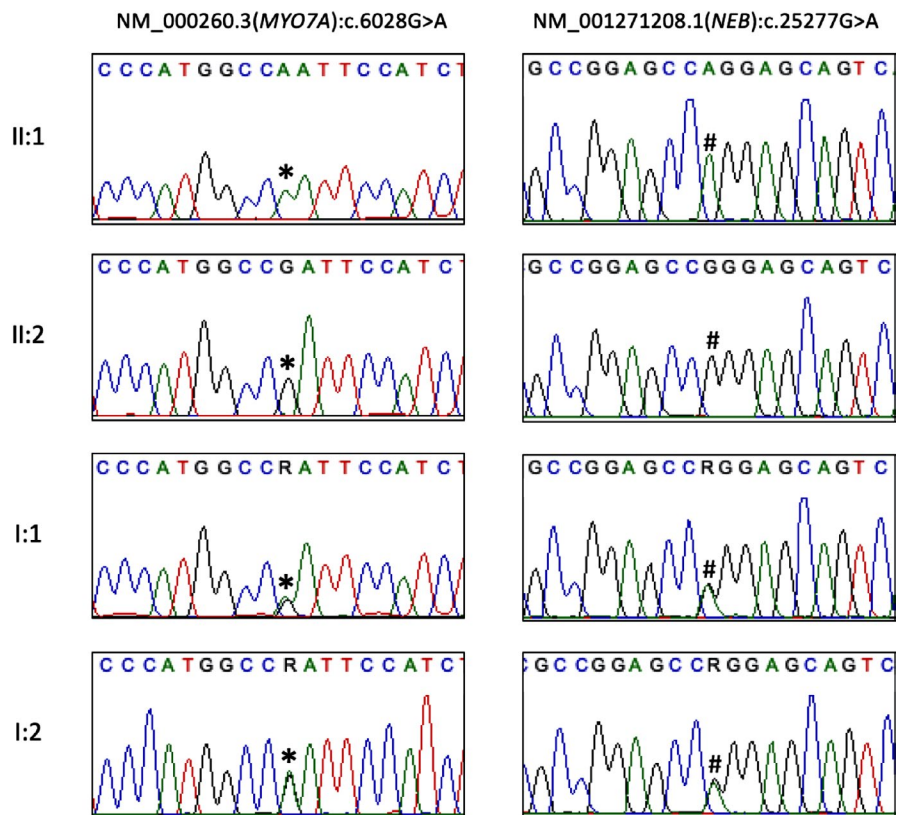


FIGURE 3 *MYO7A* and *NEB* segregation studies. Partial electropherograms showing homozygous *MYO7A* (*) NM_000260.3:c.6028G>A (exon 44), and *NEB* (#) NM_001271208.1:c.25277G>A (exon 181) variants in the proband (II:1) and confirming the heterozygous carrier status of both parents (I:1 and I:2), as well as the absence of variants in both genes in the healthy sister (II:2)

previous analysis of a panel for syndromic congenital deafness, which comprised 175 variants, among 14 genes, *MYO7A* included. *MYO7A* pathogenic variants are a well-known cause of Usher syndrome type 1 B (USH1B, OMIM#276900), a genetically heterogeneous autosomal recessive disorder mainly characterized by eyes/vision and hearing impairment.^{9,30} USH1B patients usually present hearing loss, retinitis pigmentosa, vision loss, and delayed motor development.^{31–33} The variant c.1007G>A with CADD score of 24.1, targets a moderately conserved amino acid residue, has been reported in homozygosity in two individuals (gnomAD) and is classified as VOUS or likely benign (ClinVar RCV000765013.1/RCV000710328.1/RCV000036038.4), whereas c.6028G>A with a CADD score of 27.3, has been reported as likely pathogenic/pathogenic (ClinVar RCV000666616.1/RCV000763284.1) and has no represented homozygosity, indicating a pathogenic impact. Segregation studies, by Sanger sequencing, confirmed the presence of this pathogenic variant in heterozygosity in both parents, and the absence in the healthy sister (Figure 3). Although the kyphosis presented by our proband could be, at least partially, explained by the vestibular impairment, the other musculoskeletal complaints are not associated with Usher syndrome.³⁴ *NEB* pathogenic variants are implicated in the nemaline myopathy type 2 (NEM2, OMIM#256030), mainly characterized by early-onset muscle weakness, predominately in proximal limb muscles with a high variability, ranging from mild to severe.³⁵ Moreover, patients with a mild muscle involvement, despite onset in childhood, can be misclassified as adult/late-onset form, due to heterogeneousness of both the clinical presentation and the disease progression. The majority of the NEM2 adult patients, which represent 4% of *NEB* cases,³⁶ develop generalized weakness around the second or the fifth decade of age, without any previous symptom. Other clinical features may also be present, including, cardiomyopathy, the "dropped head" syndrome and severe weakness of neck extension with or without neck flexor weakness. The identified *NEB* gene homozygous missense variant NM_001271208.1:c.25277G>A, p.(Arg8426Gln) with CADD score of 23.5, minor allele frequency 2.91e–5 (gnomAD) has been reported as VOUS (ClinVar, RCV000686525.1). However, both data resources have no represented homozygosity for p.(Arg8426Gln), suggesting a likely pathogenic effect. Segregation studies, by Sanger sequencing, confirmed the presence of this variant in heterozygosity in both parents and the absence in the healthy sister (Figure 3). The highly conserved 8426 Arginine residue is located at the *NEB* C-terminus, a region responsible for Z-disk anchoring and protein interactions.³⁷ Previous studies reported that *NEB* frameshift changes are predicted to truncate protein significantly, while missense variants compromise the interaction with other proteins, such as actin and tropomyosin, leading to the myopathy.^{38,39} Likewise, we hypothesize that mutated Nebulin is mislocated or unable to interact with other critical muscular proteins thus compromising the normal

muscle functioning and causing the milder muscular course observed in our proband.

5 | DISCUSSION

Herein, we report a patient with a complex phenotype, with vision, hearing and muscle involvement caused by variants in *MYO7A* and *NEB* genes. To enable a thorough and comprehensive analysis of patients' phenotype, HPO terminology was used to describe the clinical features. HPO has been increasingly used as a gold-standard resource, allowing the integration of clinical data across the scientific community and translational research, improving disease diagnosis yield.^{14,15}

Each one of the variants, *per se*, does not explain the overall spectrum of the proband's clinical phenotype. However, the cumulative effect of the two molecular defects could cause this complex clinical presentation. *MYO7A* variant (c.6028G>A) is implicated in the visual and hearing impairments, while the skeletal muscle involvement and some dysmorphisms, such as hypertelorism and high palate, could be caused by the *NEB* variant (c.25277G>A).^{9,30,35} Interestingly, a panel for syndromic congenital deafness, including *MYO7A* variants, does not include those identified here, which led the authors to conclude that this is not a cost-effective approach, particularly deafness gene panels targeting specific variants. There is an increase in the number of patients described with a combination of pathogenic variants in distinct genes, mostly due to the use of genome-wide technologies. The presence of two rare conditions, rather than one disease with phenotypic expansion, is not an unusual finding, particularly, but not exclusively, in consanguineous families. In fact, recent estimates revealed that 7% of the molecularly diagnosed patients carry a combination of two pathogenic variants implicated in distinct Mendelian disorders.¹⁰ Therefore, care should be taken to publish new "broaden" phenotypes in well-established syndromes particularly those that include "skeletal or muscle changes." This report also highlights that a precise clinical characterization, and consequently a correct molecular diagnosis, might be hampered by the noncoincident age of onset of each condition, as well as adult-onset disorders, progressive diseases, and mild phenotypes. In conclusion, we show the first molecular diagnosis of two Mendelian diseases unraveled by ES data homozygosity mapping, in a patient with a clinical diagnosis of Usher syndrome and unrelated muscle complaints. The presence of two clinical entities has allowed an ophthalmological and otorhinolaryngological follow-up as well as referral for neuromuscular consultation for proper monitoring of the skeletal muscle complaints. Furthermore, this report also emphasizes the limitations of phenotype-targeted gene panels as a first-tier test and demonstrates that introducing exome scale sequencing into the clinical workflow can shorten the diagnostic odyssey and provide clinical utility and potential tailored therapeutic interventions.

ACKNOWLEDGMENTS

The authors express their sincere gratitude to this family. UMIB is supported by National Funds through the FCT—Fundação para a Ciência e a Tecnologia (Portuguese national funding agency for science, research and technology) in the framework of the UID/Multi/00215/2019 project—Unit for Multidisciplinary Research in Biomedicine—UMIB/ICBAS/UP. Nuno Maia and Paula Jorge were awarded with Centro Hospitalar Universitário do Porto, 2017 PhD DEFI-CHUP and DEFI—2015 (145/12) grants, respectively.

CONFLICT OF INTEREST

None declared.

AUTHOR CONTRIBUTIONS

NM: conceived and designed the study, performed molecular studies, and involved in drafting and writing. ARS: collected the clinical data and involved in writing. AMF: involved in clinical assessment and medical data interpretation. IM: analyzed the data and involved in critical reviewing of the manuscript. AG: performed HUMARA studies and involved in the manuscript review. RS and MMP: involved in critical reviewing of the manuscript. APMB: supervised ES studies and further analysis, and involved in the manuscript final critical revision. PJ: supervised molecular and *in silico* analyses, and involved in drafting and manuscript revisions. All authors read and gave approval to the final version of the manuscript.

ETHICAL APPROVAL

Proband's legal representative signed informed consent for ID research and DNA biobanking, and for the publication of photographs. This study has been approved by the medical ethical committee of the Centro Hospitalar Universitário do Porto (CHUP, EPE)—REF 2015.196 (168-DEFI/157-CES)—and ICBAS, UP—PROJETO N° 129/2015.

ORCID

Nuno Maia  <https://orcid.org/0000-0003-3274-2474>

Ana Rita Soares  <https://orcid.org/0000-0001-7817-9889>

Ana Maria Fortuna  <https://orcid.org/0000-0002-1296-5366>

[org/0000-0002-1296-5366](https://orcid.org/0000-0002-1296-5366)

Isabel Marques  <https://orcid.org/0000-0002-3561-1288>

Ana Gonçalves  <https://orcid.org/0000-0002-3917-2323>

Rosário Santos  <https://orcid.org/0000-0002-8594-6377>

Manuel Melo Pires  <https://orcid.org/0000-0002-0046-6455>

[org/0000-0002-0046-6455](https://orcid.org/0000-0002-0046-6455)

Arjan P. M. de Brouwer  <https://orcid.org/0000-0002-2131-0484>

[org/0000-0002-2131-0484](https://orcid.org/0000-0002-2131-0484)

Paula Jorge  <https://orcid.org/0000-0002-6507-222X>

REFERENCES

- Vissers LE, Gilissen C, Veltman JA. Genetic studies in intellectual disability and related disorders. *Nat Rev Genet.* 2016;17(1):9-18.
- Monroe GR, Frederix GW, Savelberg SM, et al. Effectiveness of whole-exome sequencing and costs of the traditional diagnostic trajectory in children with intellectual disability. *Genet Med.* 2016;18(9):949-956.
- Rump P, Jazayeri O, van Dijk-Bos KK, et al. Whole-exome sequencing is a powerful approach for establishing the etiological diagnosis in patients with intellectual disability and microcephaly. *BMC Med Genomics.* 2016;9(1):7.
- Gazzo A, Raimondi D, Daneels D, et al. Understanding mutational effects in digenic diseases. *Nucleic Acids Res.* 2017;45(15):e140.
- Prasun P, Pradhan M, Agarwal S. One gene, many phenotypes. *J Postgrad Med.* 2007;53(4):257-261.
- Ehrenberg M, Pierce EA, Cox GF, Fulton AB. CRB1: one gene, many phenotypes. *Semin Ophthalmol.* 2013;28(5-6):397-405.
- Chen X, Sheng X, Liu Y, et al. Distinct mutations with different inheritance mode caused similar retinal dystrophies in one family: a demonstration of the importance of genetic annotations in complicated pedigrees. *J Transl Med.* 2018;16(1):145.
- Dong H, Nebert DW, Bruford EA, Thompson DC, Joenje H, Vasiliou V. Update of the human and mouse Fanconi anemia genes. *Hum Genomics.* 2015;9:32.
- Millan JM, Aller E, Jaijo T, Blanco-Kelly F, Gimenez-Pardo A, Ayuso C. An update on the genetics of usher syndrome. *J Ophthalmol.* 2011;2011:417217.
- Papadimitriou S, Gazzo A, Versbraegen N, et al. Predicting disease-causing variant combinations. *Proc Natl Acad Sci USA.* 2019;116(24):11878-11887.
- Alkuraya FS. Homozygosity mapping: one more tool in the clinical geneticist's toolbox. *Genet Med.* 2010;12(4):236-239.
- Wakeling MN, Laver TW, Wright CF, et al. Homozygosity mapping provides supporting evidence of pathogenicity in recessive Mendelian disease. *Genet Med.* 2019;21(4):982-986.
- Gazzo AM, Daneels D, Cilia E, et al. DIDA: a curated and annotated digenic diseases database. *Nucleic Acids Res.* 2016;44(D1):D900-D907.
- Kohler S, Schulz MH, Krawitz P, et al. Clinical diagnostics in human genetics with semantic similarity searches in ontologies. *Am J Hum Genet.* 2009;85(4):457-464.
- Kohler S, Vasilevsky NA, Engelstad M, et al. The human phenotype ontology in 2017. *Nucleic Acids Res.* 2017;45(D1):D865-D876.
- Miller SA, Dykes DD, Polesky HF. A simple salting out procedure for extracting DNA from human nucleated cells. *Nucleic Acids Res.* 1988;16(3):1215.
- Cingolani P, Platts A, Le Wang L, et al. A program for annotating and predicting the effects of single nucleotide polymorphisms, SnpEff: SNPs in the genome of *Drosophila melanogaster* strain w1118; iso-2; iso-3. *Fly (Austin).* 2012;6(2):80-92.
- Kircher M, Witten DM, Jain P, O'Roak BJ, Cooper GM. A general framework for estimating the relative pathogenicity of human genetic variants. *Nat Genet.* 2014;46(3):310-315.
- Shapiro MB, Senapathy P. RNA splice junctions of different classes of eukaryotes: sequence statistics and functional implications in gene expression. *Nucleic Acids Res.* 1987;15(17):7155-7174.
- Yeo G, Burge CB. Maximum entropy modeling of short sequence motifs with applications to RNA splicing signals. *J Comput Biol.* 2004;11(2-3):377-394.
- Reese MG, Eeckman FH, Kulp D, Haussler D. Improved splice site detection in Genie. *J Comput Biol Fall.* 1997;4(3):311-323.

22. Pertea M, Lin X, Salzberg SL. GeneSplicer: a new computational method for splice site prediction. *Nucleic Acids Res.* 2001;29(5):1185-1190.
23. den Dunnen JT, Antonarakis SE. Mutation nomenclature extensions and suggestions to describe complex mutations: a discussion. *Hum Mutat.* 2000;15(1):7-12.
24. Allen RC, Zoghbi HY, Moseley AB, Rosenblatt HM, Belmont JW. Methylation of HpaII and HhaI sites near the polymorphic CAG repeat in the human androgen-receptor gene correlates with X chromosome inactivation. *Am J Hum Genet.* 1992;51(6):1229-1239.
25. Amos-Landgraf JM, Cottle A, Plenge RM, et al. X chromosome-inactivation patterns of 1,005 phenotypically unaffected females. *Am J Hum Genet.* 2006;79(3):493-499.
26. Abidi F, Miano M, Murray J, Schwartz C. A novel mutation in the PHF8 gene is associated with X-linked mental retardation with cleft lip/cleft palate. *Clin Genet.* 2007;72(1):19-22.
27. Koivisto AM, Ala-Mello S, Lemmela S, Komu HA, Rautio J, Jarvela I. Screening of mutations in the PHF8 gene and identification of a novel mutation in a Finnish family with XLMR and cleft lip/cleft palate. *Clin Genet.* 2007;72(2):145-149.
28. Laumonnier F, Holbert S, Ronce N, et al. Mutations in PHF8 are associated with X linked mental retardation and cleft lip/cleft palate. *J Med Genet.* 2005;42(10):780-786.
29. Edvardson S, Yi JK, Jalas C, et al. Deficiency of the alkaline ceramidase ACER3 manifests in early childhood by progressive leukodystrophy. *J Med Genet.* 2016;53(6):389-396.
30. Jouret G, Poirsier C, Spodenkiewicz M, et al. Genetics of Usher syndrome: new insights from a meta-analysis. *Otol Neurotol.* 2019;40(1):121-129.
31. Adato A, Weil D, Kalinski H, et al. Mutation profile of all 49 exons of the human myosin VIIA gene, and haplotype analysis, in Usher 1B families from diverse origins. *Am J Hum Genet.* 1997;61(4):813-821.
32. Li Y, Su J, Ding C, Yu F, Zhu B. Identification of four novel mutations in MYO7A gene and their association with nonsyndromic deafness and Usher Syndrome 1B. *Int J Pediatr Otorhinolaryngol.* 2019;120:166-172.
33. Ramzan K, Al-Owain M, Huma R, et al. Utility of whole exome sequencing in the diagnosis of Usher syndrome: report of novel compound heterozygous MYO7A mutations. *Int J Pediatr Otorhinolaryngol.* 2018;108:17-21.
34. Caldani S, Bucci MP, Tisne M, Audo I, Van Den Abbeele T, Wiener-Vacher S. Postural instability in subjects with Usher syndrome. *Front Neurol.* 2019;10:830.
35. Lehtokari VL, Kiiski K, Sandaradura SA, et al. Mutation update: the spectra of nebulin variants and associated myopathies. *Hum Mutat.* 2014;35(12):1418-1426.
36. Ryan MM, Schnell C, Strickland CD, et al. Nemaline myopathy: a clinical study of 143 cases. *Ann Neurol.* 2001;50(3):312-320.
37. Chu M, Gregorio CC, Pappas CT. Nebulin, a multi-functional giant. *J Exp Biol.* 2016;219(Pt 2):146-152.
38. Marttila M, Hanif M, Lemola E, et al. Nebulin interactions with actin and tropomyosin are altered by disease-causing mutations. *Skelet Muscle.* 2014;4:15.
39. Lehtokari VL, Pelin K, Sandbacka M, et al. Identification of 45 novel mutations in the nebulin gene associated with autosomal recessive nemaline myopathy. *Hum Mutat.* 2006;27(9):946-956.
40. Kent WJ, Sugnet CW, Furey TS, et al. The human genome browser at UCSC. *Genome Res.* 2002;12(6):996-1006.

SUPPORTING INFORMATION

Additional supporting information may be found online in the Supporting Information section.

How to cite this article: Maia N, Soares AR, Fortuna AM, et al. Usher syndrome and Nebulin-associated myopathy in a single patient due to variants in MYO7A and NEB. *Clin Case Rep.* 2020;8:2476–2482. <https://doi.org/10.1002/ccr3.3146>